Real-space observation of quasicrystalline Sn monolayer formed on the fivefold surface of icosahedral Al—Cu—Fe quasicrystal

H. R. Sharma,[1,2,*] M. Shimoda,[1,2] A. R. Ross,[3] T. A. Lograsso,[3] and A. P. Tsai[1,2,4]
[1]*National Institute for Materials Science, 1-2-1 Sengen, Tsukuba, Ibaraki, 305-0047, Japan*
[2]*Solution-Oriented Research for Science and Technology (SORST), Japan Science and Technology Agency, Kawaguchi, Saitama, 332–0012, Japan*
[3]*Department of Materials Science and Engineering, Ames Laboratory, Ames, Iowa 50011, USA*
[4]*Institute of Multidisciplinary Research for Advanced Materials, Tohoku University, Sendai, 980-8577, Japan*
(Received 16 December 2004; published 14 July 2005)

We investigate a thin Sn film grown at elevated temperatures on the fivefold surface of an icosahedral Al—Cu—Fe quasicrystal by scanning tunneling microscopy (STM). At about one monolayer coverage, the deposited Sn is found to form a smooth film of height consistent with one-half of the lattice constant of the bulk Sn. Analysis based on the Fourier transform and autocorrelation function derived from high-resolution STM images reveals that Sn grows pseudomorphically and hence exhibits a quasicrystalline structure.

DOI: 10.1103/PhysRevB.72.045428 PACS number(s): 61.44.Br, 68.55.−a, 68.37.Ef

I. INTRODUCTION

Quasicrystals are intermetallic compounds of specific stoichiometry[1] possessing aperiodic long-range order often associated with crystallographically forbidden rotational symmetries such as five- or tenfold axes. Due to the success in the growth of large single-grain samples, surface studies of this type of solid with various experimental techniques have become possible and significant progress has been made in the surface preparation and characterization (see, for example, Refs. 2 and 3 and references therein). Recently, attention has been given to thin-film growth on these complex surfaces. The main goal of film growth studies is to fabricate epitaxial quasicrystalline single-element films (pseudomorphic films). Such an artificial structure could potentially be used to study the exclusive influence of quasiperiodicity on the associated physical properties, i.e., independently of the complex alloy composition of stable bulk phases.

Most of the attempts to fabricate quasicrystalline single-element films so far resulted in either periodic films exhibiting orientational relationship with the substrate [4–10] or films with no long-range order.[11] Only a limited number of systems are found to yield films with quasicrystalline long-range order. Franke *et al.* characterized the reciprocal space of Bi and Sb films grown at 300 °C on decagonal Al—Ni—Co and icosahedral (*i*) Al—Pd—Mn surfaces by low-energy electron diffraction and He atom scattering and showed that both Bi and Sb yield highly ordered quasicrystalline monolayer.[12,13] However, no real-space images of such monolayers have been reported so far.

A recent report on Cu growth on the *i*-Al—Pd—Mn surface by Ledieu *et al.* reveals that Cu does not show pseudomorphic growth for coverages up to three monolayers but develops rows arranged in quasiperiodic order for higher coverages.[14] However, the atomic structure of Cu in the rows could not be resolved, making it impossible to fully establish the structural relationship between the substrate and the film. Another report by Cai *et al.* on Al growth on the fivefold *i*-Al—Cu—Fe surface suggests that Al yields pseudomorphic islands in the submonolayer regime but as coverage increases three-dimensional islands are formed.[15]

In this paper, we present an analysis of a thin Sn film grown at 300–350 °C on the fivefold *i*-Al—Cu—Fe surface. Scanning tunneling microscopy (STM) images of the film reveal that the deposited Sn grows pseudomorphically at about monolayer coverage and hence exhibits quasicrystalline structure. To our knowledge, the present results constitute the first observation of real-space images of a pseudomorphic monolayer film formed on the quasicrystal surface.

II. EXPERIMENT

For the surface preparation of the substrate, the single-grain $Al_{63}Cu_{24}Fe_{13}$ sample[16] was cut along the fivefold plane and mechanically polished using diamond paste down to 0.25 μm. Subsequently, repeated cycles of Ar^+ sputtering (1–3 keV) and annealing (up to about 750 °C) were performed in the UHV chamber (base pressure 1×10^{-10} mbar). The cleaning process was repeated until no oxygen was detectable by x-ray photoemission spectroscopy (XPS).

Sn was deposited on the thus prepared surface in a connected UHV chamber by using a liquid-nitrogen-cooled evaporator with a tungsten basket. The temperature of the sample was kept at 300–350 °C during deposition. After the deposition, the sample was transferred into the STM chamber without exposure to air and STM data were recorded by using an Omicron room temperature STM. Images were recorded in constant-current mode.

The coverage was estimated by measuring XPS core level spectra for Al 2*s*, Cu $2p_{3/2}$, and Sn $3d_{5/2}$ from the Sn-covered surface. The coverage estimated by XPS was confirmed by STM data at about one monolayer (ML) coverage. With this coverage and deposition time, the deposition rate of Sn was calculated to be ~0.25 ML/s.

III. RESULTS AND DISCUSSION

The structure of the clean fivefold *i*-Al—Cu—Fe surface used for Sn growth has been reported elsewhere.[17] Here, we

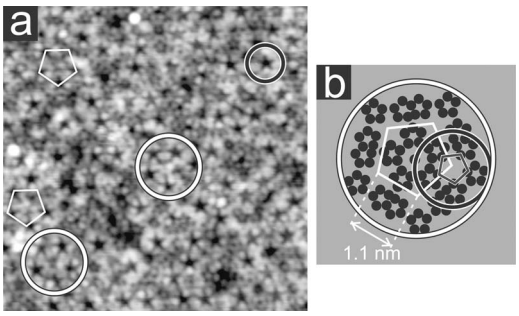

FIG. 1. (a) High-resolution image on a terrace of the clean fivefold *i*-Al—Cu—Fe surface (area $A=16\times16$ nm^2; bias voltage $V_B=1.1$ V; and tunneling current $I_T=0.25$ nA). (b) Description of the marked area in terms of atom sites (Ref. 17). Small solid circles mark sites which can be occupied by an atom or empty, depending on locations.

describe only those points that are relevant to the discussion of the film structure presented below. Scanning tunneling microscopy of the clean surface reveals large terraces separated by steps of different heights.[17] All observed step heights (h) can be obtained by linear combination of two basic heights of 0.37 nm ($=L$) and L/τ ($=S$), i.e., $h\approx mS+nL$, with $(m,n)=(1,0)$, (0,1), (1,1), (1,2), (2,2), (1,3), (2,3), (2,4), and (3,5) and $\tau=1.618\ldots$, the golden mean: a characteristic number related to pentagonal or decagonal symmetry. Terraces commonly exhibit hollow sites of pentagonal star shape (hereafter pentagonal stars) but their density differs on different terraces.[18] Such a pentagonal star is marked by a black circle in Fig. 1(a) and its description in terms of atom sites is shown in Fig. 1(b).[17] The size of these pentagonal stars is about 0.5 nm [i.e., the edge length of the black pentagon, Fig. 1(b)]. The nearest- and next-nearest-neighbor distances of the pentagonal stars are generally $1.1(\sigma=0.1)$ nm and $1.9(\sigma=0.1)$ nm, respectively, which are roughly related by τ (σ is the standard deviation). In some parts of terraces, their centers constitute the vertices of a pentagon [marked by white circles or pentagons in Fig. 1(a)]. The distances between the next and second next corners of the pentagon correspond to the quoted nearest- and next-nearest-neighbor distances of the pentagonal stars. The identical arrangement of the pentagonal stars can be identified on different terraces, but their density differs.

The STM image of the Sn-covered surface at about 1 ML coverage is given in Figs. 2(a) and 2(b). Terraces are found to be almost completely covered by a smooth film. Only a small area of terraces is bare [mainly close to the step edges, for instance, the bright part on the top and middle terraces in Fig. 2(b)). This enabled us to identify the steps associated with the film. These steps are indicated by arrows in Figs. 2(a) and 2(b) and can be clearly seen in the three-dimensional 3D view of the image in Fig. 2(b). The distribution of the measured z values in the immediate vicinity of these steps reveals the step height of $0.15(\sigma=0.01)$ nm. This height is close to one-half of the lattice constant of tetragonal Sn along the c axis [$c/2=0.1591$ nm (Ref. 19)]. The consistency of the step height with the lattice constant of Sn as well as the fact that the 0.15-nm-high steps do not appear on the clean surface confirms that these steps are associated with the Sn film.

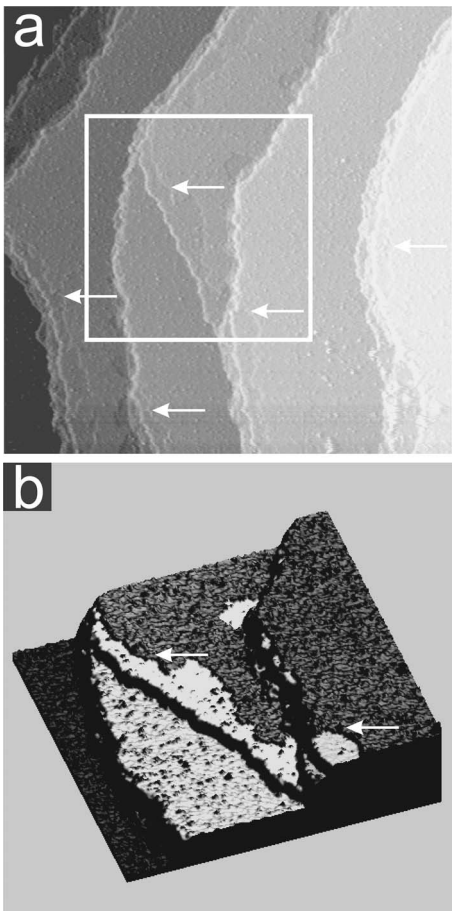

FIG. 2. STM images of the Sn-covered fivefold *i*-Al—Cu—Fe surface for about 1 ML coverage. Arrows point to steps associated with Sn film. ($V_B=2.8$ V and $I_T=0.2$ nA.) (a) Image is presented in derivative form to highlight steps ($A=300\times300$ nm^2). (b) 3D view of framed area of image (a).

A high-resolution image of the film is shown in Fig. 3(a). A Fourier transform derived from the STM image shows spots (maxima) with a near tenfold symmetry [Fig. 3(b)]. The slight modification observed in the Fourier transform from a perfect tenfold symmetry is attributed to the distortion of the STM images which is mainly due to thermal drift during scanning and/or limits in the piezo calibration. The successive maxima in the Fourier transform are located at 1.1, 1.8, and 3.0 nm^{-1} from the center. (The given values are the average distances of ten individual maxima degenerated into a distorted ring.) The ratio of these values is $\sim1:\tau:\tau^2$. The τ-scaling relation of the maxima positions reflects the quasiperiodic order of the film.

The autocorrelation function derived from high-resolution STM images yields maxima which extend up to the maximum distance within the STM image, revealing long-range order within the experimentally probed length scale [Fig. 3(c)]. Two types of spots are predominantly identified in the autocorrelation function: broad spots of diffuse nature and small sharp spots. These two types of spots together form a squeezed decagon, especially close to the center [marked by

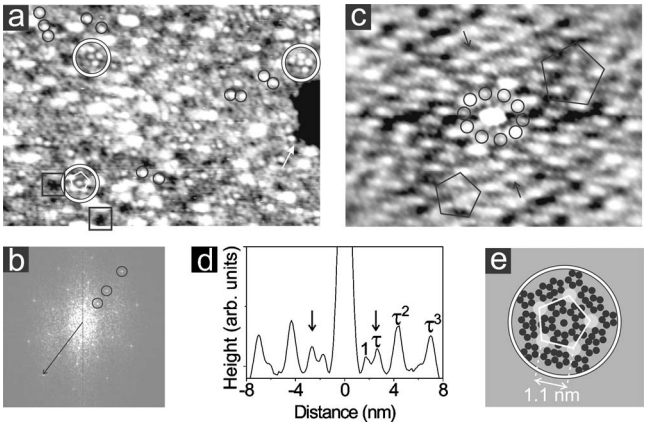

FIG. 3. (a) High-resolution image of Sn film for about 1 ML coverage ($A=35\times24$ nm^2, $V_B=1.2$ V, and $I_T=0.2$ nA). Representatives of repeating motifs are marked by circles of different colors and squares. Arrow points to the step associated with Sn film. (b) Fourier transform derived from image (a). Arrow marks about 3.0 nm^{-1}. The successive maxima are marked by circles as a guide for eyes. (c) Autocorrelation function derived from image (a) ($A=33\times24$ nm^2). (d) Height profile along the line pointed by arrows in autocorrelation function (c). Peaks indicated by arrows correspond to maxima marked by circles in autocorrelation function (c). Peaks are located at τ-scaling distance. (e) Depiction of possible location of dotlike protrusions observed on the film, marked by circles in image (a). Gray and black solid circles represent the location of Sn protrusions and the substrate atom sites, respectively.

circles in Fig. 3(c)]. Height profiles along the lines joining the center and the vertices of the decagon show τ-scaling spacing of the spots [Fig. 3(d)]. The τ-scaling spacing as well as observed pentagonal features in the autocorrelation function [marked by pentagons in Fig. 3(c)] demonstrates the quasiperiodic nature of the film in agreement with the conclusion drawn from the Fourier transform of the film.

The film consists of fine structure [gray part in Fig. 3(a)], protrusions (brighter features), and depression (black part). Identical pentagonal features can be directly identified on the film; see, for example, pentagonal depression marked by squares and pentagons marked by white circles in Fig. 3(a). The film exhibits roughness as compared to the substrate. A typical root mean square of the measured z values of the Sn-covered surface is about 0.04 nm, while that of the clean surface is about 0.02 nm.

Many of the protrusions observed on the image are of relatively homogeneous size and shape [dotlike protrusions; representatives are marked by black circles in Fig. 3(a)], while the rest are relatively larger and of irregular shape. We employed a "height filter" to select the protrusions. A portion of the STM image given in Fig. 3(a) after height filtering is shown in Fig. 4(a). Fourier transform of the filtered image still shows a weak tenfold pattern [Fig. 4(b)], suggesting that the distribution of the protrusions is ordered, not random. This indicates that the protrusions are located at specific sites of the substrate.

The following observations suggest that pentagonal stars of the substrate, discussed in the beginning of this section, are the most probable sites where the dotlike protrusions are

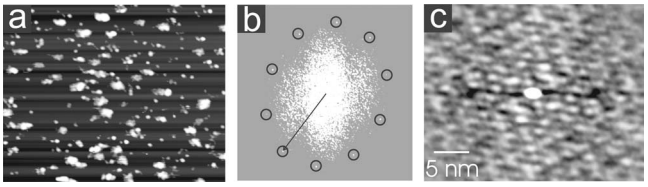

FIG. 4. (a) A portion of image in Fig. 3(a) after height filtering ($A=31\times24$ nm^2). (b) Fourier transform of the filtered image. Arrow marks about 3.0 nm^{-1}. (c) Autocorrelation function of the filtered image ($A=31\times24$ nm^2).

located as depicted in Fig. 3(e). (i) The dotlike protrusions are found to be distributed over the terraces like the pentagonal hollow sites of the substrate. The nearest- and next-nearest-neighbor distances of most of these protrusions are $1.1(\sigma=0.1)$ nm and $1.8(\sigma=0.1)$ nm which are consistent with those of the pentagonal stars. (ii) Different terraces exhibit these protrusions located at the vertices of a pentagon, as marked by white circles in Fig. 3(a). The edge length of the pentagon is equivalent to the nearest-neighbor distance of the protrusions. This arrangement is similar to that of the pentagonal stars identified on the substrate [compare white pentagons in Figs. 1 and 3(a)]. The density of the pentagonal arrangement of the protrusions differs on different terraces like the pentagonal arrangement of the pentagonal stars of the substrate. (iii) The lateral size of the protrusions roughly matches the size of the pentagonal stars. (iv) It is known from a number of previous studies that pentagonal hollow sites act as adsorption and nucleation sites.[20,15] These reports support the present observations.

As we described above the film possesses fine structure and protrusions. We also demonstrated that both the film as a whole and the protrusions alone yield a tenfold Fourier transform. The Fourier transform of both produces spots at $k=3.0$ nm^{-1}, the outermost spots pointed out by arrows in Figs. 3(b) and 4(b), but inner spots are visible only in the Fourier transform of the film. This suggests that the film exhibits a higher degree of quasiperiodic order with the fine structure part rather than with the protrusions alone. A clear difference is observed between the autocorrelation function of the film and that of the protrusions. We showed above that the autocorrelation function of the film exhibits broad diffuse spots and small sharp spots. The broad diffuse spots are reproduced in the autocorrelation function of the protrusions, but small spots do not appear [Fig. 4(c)]. This implies that small spots observed in the autocorrelation function of the film result mainly from the fine structure part. These small spots combined with the broad spots show τ-scaling distribution as explained above. This reveals that both the fine structure and the protrusions constitute parts of the monolayer film that demonstrate excellent quasicrystalline long-range order.

In summary, we find that the deposited Sn forms a smooth film. The analysis of the step height reveals a monatomic height of the film. Both the Fourier transform and autocorrelation function derived from high-resolution STM images strongly suggest that the film adopts quasicrystalline long-range order of the substrate.

IV. CONCLUSIONS

We presented an analysis of a thin Sn film grown at elevated temperatures on the fivefold surface of an *i*-Al—Cu—Fe quasicrystal investigated by scanning tunneling microscopy. We demonstrated that monolayer coverage yields a smooth film of height consistent with one-half of the lattice constant of the bulk Sn. The film's structure was found to yield a tenfold Fourier transform with maxima located at τ-scaling positions. The autocorrelation function derived from high-resolution STM images exhibits maxima extending up to maximum distance within the STM image, revealing long-range order of the film. The maxima in the autocorrelation function also exhibit τ-scaling distribution. With these results we suggested that Sn grows pseudomorphically and hence exhibits quasicrystalline order. This finding has opened up the opportunity to investigate the exclusive relationship between quasiperiodicity and associated physical properties independently of the complex alloy composition of bulk phases.

ACKNOWLEDGMENTS

This work was partially supported by JST Solution-Oriented Research for Science and Technology (SORST) and JSPS Grants-in-Aid for Scientific Research. One of the authors (H.R.S.) would like to thank the Japan Society for the Promotion of Science (JSPS) for the fellowship grant (Fellow IDNo. P04558). We would like to thank W. Theis at FU Berlin and V. Fournée at CNRS Nancy for critical reading of the manuscript and valuable suggestions.

*Corresponding author. Email address: hemraj.sharma@nims.go.jp

[1] A. P. Tsai, in *Physical Properties of Quasicrystals*, edited by Z. M. Stadnik (Springer, Berlin, 1999).
[2] R. McGrath, J. Ledieu, E. J. Cox, and R. D. Diehl, J. Phys.: Condens. Matter **14**, R119 (2002).
[3] P. A. Thiel, A. I. Goldman, and C. J. Jenks, in *Physical Properties of Quasicrystals*, edited by Z. M. Stadnik (Springer, Berlin, 1999).
[4] B. Bolliger, V. E. Dmitrienko, M. Erbudak, R. Lüscher, and H.-U. Nissen, Phys. Rev. B **63**, 052203 (2000).
[5] M. Shimoda, T. J. Sato, A. P. Tsai, and J. Q. Guo, Phys. Rev. B **62**, 11288 (2000).
[6] M. Shimoda, J. Q. Guo, T. J. Sato, and A. P. Tsai, Surf. Sci. **482–485**, 784 (2001).
[7] M. Shimoda, J. Q. Guo, T. J. Sato, and A. P. Tsai, Jpn. J. Appl. Phys., Part 1 **40**, 6073 (2001).
[8] M. Shimoda, T. J. Sato, A. P. Tsai, and J. Q. Guo, Surf. Sci. **507–510**, 276 (2002).
[9] M. Shimoda, T. J. Sato, A. P. Tsai, and J. Q. Guo, J. Alloys Compd. **342**, 441 (2002).
[10] M. Shimoda, Prog. Surf. Sci. **75**, 87 (2004).
[11] H. R. Sharma, M. Shimoda, V. Fournée, A. R. Ross, T. A. Lograsso, and A. P. Tsai, Appl. Surf. Sci. **241**, 256 (2005).
[12] K. J. Franke, H. R. Sharma, W. Theis, P. Gille, P. Ebert, and K. H. Rieder, Phys. Rev. Lett. **89**, 156104 (2002).
[13] W. Theis, H. R. Sharma, K. J. Franke, and K. H. Rieder, in *Quasicrystals, Structure and Physical Properties*, edited by H.-R. Trebin (Wiley-VCH, Berlin, 2003).
[14] J. Ledieu, J. T. Hoeft, D. E. Reid, J. Smerdon, R. D. Diehl, T. A. Lograsso, A. R. Ross, and R. McGrath, Phys. Rev. Lett. **92**, 135507 (2004).
[15] T. Cai, J. Ledieu, R. McGrath, V. Fournée, T. Lograsso, A. Ross, and P. Thiel, Surf. Sci. **526**, 115 (2003).
[16] C. J. Jenks *et al.*, *Proceedings of the 6th International Conference on Quasicrystals*, World Scientific, 1998.
[17] H. R. Sharma, V. Fournée, M. Shimoda, A. R. Ross, T. A. Lograsso, A. P. Tsai, and A. Yamamoto, Phys. Rev. Lett. **93**, 165502 (2004).
[18] J. Ledieu and R. McGrath, J. Phys.: Condens. Matter **15**, S3113 (2003).
[19] V. T. Deshpande and D. B. Sirdeshmukh, Acta Crystallogr. **14**, 355 (1961).
[20] J. Ledieu, C. A. Muryn, G. Thornton, R. D. Diehl, T. A. Lograsso, D. W. Delaney, and R. McGrath, Surf. Sci. **472**, 89 (2001).